# State-to-state $N_2(A\ ^3\Sigma_u^+)$ energy-pooling reactions. I. The formation of $N_2(C\ ^3\Pi_u)$ and the Herman infrared system

Lawrence G. Piper
*Physical Sciences Inc., Research Park, P.O. Box 3100, Andover, Massachusetts 01810*

(Received 13 July 1987; accepted 15 September 1987)

We have studied the formation of $N_2(C\ ^3\Pi_u, v = 0\text{–}4)$ and the nitrogen Herman infrared system, $v' = 2,3$, in energy pooling reactions between $N_2(A\ ^3\Sigma_u^+, v' = 0\text{–}1)$. Our results indicate rate coefficients of $(1.5 \pm 0.4)$ and $(1.5 \pm 0.5) \times 10^{-10}$ cm$^3$ molecule$^{-1}$ s$^{-1}$ for formation of $N_2(C\ ^3\Pi_u, v' = 0\text{–}4)$ from the energy pooling of two $N_2(A,v' = 0)$ molecules and for a $v' = 0$ and a $v' = 1$ molecule, respectively. We did not see evidence of significant $N_2(C)$ formation in energy pooling between two $N_2(A,v' = 1)$ molecules ($k < 5 \times 10^{-11}$ cm$^3$ molecule$^{-1}$ s$^{-1}$). $N_2(A,v' = 0)$ energy pooling produces *only* $v' = 3$ of the Herman infrared system with a rate coefficient of $\geqslant (8.1 \pm 2.3) \times 10^{-11}$ cm$^3$ molecule$^{-1}$ s$^{-1}$. Energy pooling between $N_2(A,v' = 0)$ and $N_2(A,v' = 1)$ produces *only* $v' = 2$ of the Herman infrared system with a rate coefficient $\geqslant (9.9 \pm 2.9) \times 10^{-11}$ cm$^3$ molecule$^{-1}$ s$^{-1}$. Again, energy pooling between two $N_2(A,v' = 1)$ molecules results in no significant contributions to the Herman infrared system. The participation of $N_2(A)$ vibrational levels $\geqslant 2$, however, does result in excitation of the lower-lying vibrational levels of the Herman infrared system.

## I. INTRODUCTION

Stedman and Setser[1] first discovered energy pooling in triplet nitrogen when they observed that the intensity of nitrogen second-positive, $N_2(C\ ^3\Pi_u\text{–}B\ ^3\Pi_g)$ emission varied quadratically with the intensity of the Vegard–Kaplan, $N_2(A\ ^3\Sigma_u^+\text{–}X\ ^1\Sigma_g^+)$, emission in their reactor. They estimated the rate coefficient for energy pooling to form $N_2(C\ ^3\Pi_u)$ to be $2.1 \times 10^{-11}$ cm$^3$ molecule$^{-1}$ s$^{-1}$. In a series of investigations of time-resolved emissions in the afterglow of a pulsed nitrogen discharge, Hays *et al.*[2–4] studied $N_2(A)$ energy pooling and reported rate coefficients of $2.6 \times 10^{-10}$ for formation of $N_2(C\ ^3\Pi_u)$,[4] $0.25 \times 10^{-10}$ cm$^3$ molecules$^{-1}$ s$^{-1}$ for the formation of $N_2(C'\ ^3\Pi_u)$, and $1.1 \times 10^{-9}$ cm$^3$ molecule$^{-1}$ s$^{-1}$ for the formation of $N_2(B\ ^3\Pi_g)$.[3] In the case of the latter state, one would have to assume that their number was a lower bound, because their detection system could see only as far as $v' = 3$ of the $B$ state. Thus, if significant energy from the pooling reaction flowed into $v' = 0\text{–}2$, the rate coefficient would be somewhat larger. Subsequent work by Clark and Setser[5] confirmed a rate coefficient of about $2 \times 10^{-10}$ cm$^3$ molecule$^{-1}$ s$^{-1}$ for the production of $N_2(C\ ^3\Pi_u)$ from $N_2(A\ ^3\Sigma_u^+)$ energy pooling. They were unable, however, to see any evidence for formation of the $N_2(C'\ ^3\Pi_u)$ state. Nadler *et al.*[6] discovered in 1980 that the Herman infrared (HIR) system was populated by $N_2(A)$ energy pooling, and showed subsequently that the distribution among the vibrational levels of that state depended strongly upon the vibrational distribution of the $N_2(A)$ state.[7] They estimated a lower limit for HIR formation[6] of $2.5 \times 10^{-11}$ cm$^3$ molecule$^{-1}$ s$^{-1}$ which they have since revised upwards to $7 \times 10^{-11}$ cm$^3$ molecule$^{-1}$ s$^{-1}$.[7] They also showed that some production of the $B$ state did indeed occur, but were unable to estimate the rate coefficient for $B$-state formation because of that state's rapid quenching by nitrogen and argon. Nadler and Rosenwaks[8] have shown recently that the vibrational distribution of $N_2(C\ ^3\Pi_u)$ formed by energy pooling also changes as a function of the $N_2(A)$ vibrational distribution, but that the total excitation rate of the $C$ state appears to be independent of the vibrational distribution of $N_2(A)$.

Unpublished observations at PSI in the near infrared recorded the HIR system in $N_2(A)$ energy pooling, but failed to detect significant populations of $N_2(B)$.[9] We could not rationalize, therefore, the magnitude of the pooling rate coefficient which Hays and Oskam reported for $N_2(B)$ production. The work of Nadler *et al.*[6,7] also showed convincingly that HIR production had to be similar in magnitude to the production of $N_2(B)$. Thus, the present investigations were motivated in part by our desire to reconcile the conflict between Hays and Oskam's report, and the observations of Nadler *et al.*, and our own. We have investigated energy pooling in some detail and report here vibrational-level-specific rate coefficients for formation of $N_2(C\ ^3\Pi_u, v' = 0\text{–}4)$ and HIR $v' = 2,3$ by $N_2(A\ ^3\Sigma_u^+, v' = 0\text{–}2)$. Electronic quenching plays an important role in understanding $N_2(B\ ^3\Pi_g)$ formation. A subsequent paper covers both the excitation of $N_2(B)$ in $N_2(A)$ energy pooling as well as the electronic quenching of the $B$ state.

## II. EXPERIMENTAL

### A. Apparatus

Previous publications have described our 2 in. discharge–flow apparatus and general operating procedures in some detail.[10–16] Thus, we will give only a brief summary here. The studies all involved measuring spectra of the Vegard–Kaplan, first- and second-positive and HIR systems of molecular nitrogen in a flowing afterglow apparatus. The $N_2(A)$ is produced cleanly in the apparatus in the energy transfer reaction between argon or xenon metastables and molecular nitrogen.[17,18] A hollow-cathode discharge produces the rare gas metastables. We have generally fabricated

 0021-9606/88/010231-09$02.10  

the electrode from aluminum shim, but for some of the studies here, we used 0.002 thick tantalum shim as the electrode material. The tantalum electrodes gave about 30% more metastables and operated better at high pressures. The energy transfer reaction between metastable xenon and nitrogen produces $N_2(B\,^3\Pi_g, v' \leqslant 5)$.[19] This eliminates the possibility of contamination of the results for $N_2(C)$ and the higher vibrational levels of $N_2(B)$ by scattered light from the rare-gas-metastable/nitrogen mixing region which occurs when argon metastables are used to make $N_2(A)$. The HIR system was studied at relatively high pressures ($\gtrsim 6$ Torr) with high partial pressures of nitrogen (1 to 2 Torr) in the reactor. This procedure virtually eliminated overlapping of the HIR system by the first-positive system. The unfortunate consequence of this procedure, however, was that the high partial pressures of nitrogen relaxed the $N_2(A)$ vibration to $>95\%$ $v' = 0,1$, and thus the effects of higher vibrational levels could not be studied.

All spectra were fit by a least-squares computer program which determined the population of all emitting states in the region of spectral coverage. This procedure eliminates the uncertainties introduced by overlapping spectral bands. Because the HIR system is unassigned, one cannot *a priori* generate a synthetic spectrum for this system. We therefore used experimental spectra taken at high pressures for the basis sets in our synthetic fits. Because $N_2(A, v' = 0)$ energy pooling produces only $v' = 3$ of the HIR system, a basis set for that state could be generated cleanly. When only $v' = 0$ and 1 of $N_2(A)$ are present, only $v' = 3$ and 2 of the HIR system are produced. Thus we were able to generate a fitting basis set for $v' = 2$ of the HIR system by subtracting out the previously determined $v' = 3$ components from a spectrum containing the two levels together. These basis sets were then used in analyzing the spectra containing $N_2(B)$ to eliminate confusion from overlap between the two states.

### B. Absolute photon emission rates

The data analysis requires the measurement of absolute photon-emission rates in the reactor (see below). This section details how we calibrate our system for such measurements.

The observed signal is related to the true volume emission rate through

$$I_{\text{obs}} = I_{\text{true}} \frac{\Omega}{4\pi} \eta_\lambda T_\lambda V, \tag{1}$$

where $\Omega/4\pi$ is the effective solid angle subtended by the detection system, $\eta_\lambda$ is the quantum efficiency of the photomultiplier at the wavelength of interest, $T_\lambda$ is the transmission of the optical system (e.g., mirror reflectivities and grating efficiency) and $V$ is the observed volume of luminous gas in the reactor. The wavelength dependence of the product $(\Omega/4\pi)\eta_\lambda T_\lambda V$ is given by the relative monochromator response function $R_\lambda$. Absolute values of that product are obtained in a calibration experiment using the O/NO air afterglow at one or several specific wavelengths. Absolute values at wavelengths other than those chosen for calibration experiments are obtained by scaling with $R_\lambda$.

The relative spectral response of the monochromator was calibrated between 200 and 800 nm using standard quartz-halogen and $D_2$ continuum lamps (Optronic Laboratories Inc.). Additional confirmation of the calibration between 400 and 800 nm is obtained by scanning the air afterglow spectrum and comparing observed relative signal levels with the relative intensities given by Fontijn *et al.*[20] The absolute spectral response of the detection system is determined at 580 nm using the O/NO air afterglow as described previously.[11,13]

When atomic oxygen and nitric oxide are mixed, a continuum emission extending from 375 nm to beyond 3000 nm is observed.[20–28] The intensity of this emission is directly proportional to the product of the number densities of atomic oxygen and nitric oxide, and independent of pressure of bath gas, at least at pressures above about 0.2 Torr.[28] Thus, the volume-emission rate of the air afterglow is given by

$$I_{\text{true}} = k_\lambda [\text{O}][\text{NO}]\Delta\lambda, \tag{2}$$

where $k_\lambda$ is the air afterglow rate coefficient in units of $\text{cm}^3\ \text{molecule}^{-1}\ \text{s}^{-1}\ \text{nm}^{-1}$ and $\Delta\lambda$ is the monochromator bandwidth. Literature values for this rate coefficient span a range of more than a factor of 2,[20–26] but recent studies[25] indicate that the original work of Fontijn *et al.*[20] is probably correct at wavelengths shorter than $\approx 800$ nm. We use a value of $1.25 \times 10^{-19}\ \text{cm}^3\ \text{molecule}^{-1}\ \text{s}^{-1}\ \text{nm}^{-1}$ at $\lambda = 580$ nm. Combining Eqs. (1) and (2) gives the observed air afterglow intensity:

$$I_\lambda^{\text{O/NO}} = k_\lambda [\text{O}][\text{NO}]\Delta\lambda \frac{\Omega}{4\pi} \eta_\lambda T_\lambda V. \tag{3}$$

Air afterglow calibration experiments give a calibration factor,

$$\kappa_\lambda = \frac{I_\lambda^{\text{O/NO}}}{[\text{O}][\text{NO}]} = k_\lambda \Delta\lambda \frac{\Omega}{4\pi} \eta_\lambda T_\lambda V, \tag{4}$$

the determination of which we described previously.[11,13]

Absolute number densities of emitters are obtained by dividing absolute volume emission rates by known transition probabilities.[30] The air afterglow calibration factor $\kappa_\lambda$ and the moderately well established value of the air afterglow rate coefficient $k_\lambda$, are used to convert observed emission intensities to volume emission rates:

$$I_{\text{true}} = \frac{I_{\text{obs}} k_{\lambda_c} \Delta\lambda_c R_{\lambda_c}}{\kappa_{\lambda_c} R_{\lambda_{\text{obs}}}}, \tag{5}$$

where $\lambda_c$ represents the wavelength of the calibration experiments and $\lambda_{\text{obs}}$ is the wavelength of the transition of interest. $I_{\text{obs}}$ must be the total integrated band intensity. This is determined from the spectral fitting.

A series of calibration experiments taken over a period of time established the calibration factor $\kappa_{580}$ to $\pm 10\%$. An additional uncertainty of $\pm 25\%$ exists in the absolute value of the air-afterglow rate coefficient, $k_{580}$, Further uncertainties in the determination of the absolute photon-emission rates for $N_2(A)$ arise through the relative monochromator response function (10%) and $N_2(A)$ band transition probabilities. The uncertainty in this latter quantity is difficult to estimate. We used Shemansky's[29] transition probabilities to provide a ready basis for comparison with the existing literature. He estimated them to carry a 20% uncertainty. Our

experiments on the energy transfer between $N_2(A)$ and NO,[14] however, indicated that Shemansky's transition probabilities are likely to be 20 to 40% too large. We have chosen not to revise the $N_2(A–X)$ transition probabilities until this issue has been resolved definitively. Ignoring the uncertainty in the $N_2(A–X)$ transition probabilities, the total uncertainty in each rate coefficient, systematic and statistical combined in quadrature, will be 30%. This large figure is determined primarily by the uncertainty in the air afterglow rate coefficient.

### C. Radial density gradient corrections

In the case of the energy pooling reactions, the $N_2(A)$ and the $N_2(C,B,\mathrm{HIR})$ have radial density gradients which are different. The $N_2(A)$ radial density gradient approximately follows the form of a Bessel function of first order,[31]

$$[N_2(A)](r) = [N_2(A)]_0 J_0[\lambda(r/r_0)], \tag{6}$$

where $[N_2(A)]_0$ is the centerline number density, $r_0$ is the flow tube radius, and $\lambda = 2.405$, the first zero of $J_0(x)$. The field of view of the detector is essentially a rectangular parallelepiped across the center of the tube with height $h$, width $z$, and length $2r_0$ (see Fig. 1). We assume that variations down the axis of the flow tube, across the field of view, can be neglected. The average number density of $N_2(A)$ observed in the field of view is then

$$\langle[N_2(A)]\rangle = \frac{[N_2(A)]_0 \int_0^{r_0} J_0[\lambda(r/r_0)]\, r\theta\, dr}{\int_0^{r_0} r\theta\, dr}, \tag{7}$$

where $[N_2(A)]_0$ is the $N_2(A)$ number density in the center of the flow tube. When $r$ is less than or equal to $h/2$, $\theta$ will equal $\pi$; but when $r$ becomes greater than $h/2$, $\theta$ will be given by $\sin^{-1}(h/2r)$. Thus, each integral in Eq. (7) becomes a sum of two integrals, one between the limits of 0 and $h/2$, the other running from $h/2$ to $r_0$. For our conditions of $r_0 = 2.6$ cm and $h = 1$ cm, numerical integration gives

$$\langle[N_2(A)]\rangle = 0.601\,[N_2(A)]_0. \tag{8}$$

As we show below, the number density of $N_2(C,B,\mathrm{HIR})$ is proportional to the square of the $N_2(A)$ number density. Thus

$$\langle[N_2(C,B,\mathrm{HIR})]\rangle = k'[N_2(A)]^2 = \frac{k'[N_2A]_0^2 \int_0^{r_0} J_0^2[\lambda(r/r_0)]\, r\theta\, dr}{\int_0^{r_0} r\theta\, dr}, \tag{9}$$

where $k'$ is the energy pooling rate coefficient.

Integrating this expression in a similar manner to that given for $\langle[N_2A]\rangle$ gives

$$\langle[N_2(C,B,\mathrm{HIR})]\rangle = 0.458\, k'[N_2(A)]_0^2. \tag{10}$$

Finally, using Eq. (8) above for $[N_2(A)]_0$, we find that

$$\langle[N_2(C,B,\mathrm{HIR})]\rangle = 1.267 k'\langle[N_2(A)]\rangle^2. \tag{11}$$

This correction must be made to the data on energy pooling to extract rate coefficients. This correction factor increases as the ratio $h/r$ increases beyond unity, reaching a maximum value of 1.446 when $h/r$ equals two (Fig. 2).

## III. RESULTS

### A. $N_2(C\,^3\Pi_u, v'=0–4)$ formation in $N_2(A\,^3\Sigma_u^+, v'=0–2)$ energy pooling

The processes controlling the formation and destruction of $N_2(C)$ in the energy pooling system are:

$$N_2(A,v') + N_2(A,v'') \xrightarrow{k^{C,v}_{v'v''}} N_2(C,v) + N_2(X,v'''), \tag{12}$$

$$N_2(C,v) \xrightarrow{k^{C,v}_{\mathrm{rad}}} N_2(B) + h\nu, \tag{13}$$

where the superscript $v$ denotes the vibrational level of the $N_2(C)$ product molecule, the subscript $v$'s denote the vibrational levels of the $N_2(A)$ molecules, and $k_{\mathrm{rad}}$ is the radiative decay rate of $N_2(C)$.[30] The lifetime of $N_2(C)$ is sufficiently short ($\approx$36 ns)[30] that we may ignore electronic quenching of that state. Because of its short radiative lifetime, $N_2(C)$ is

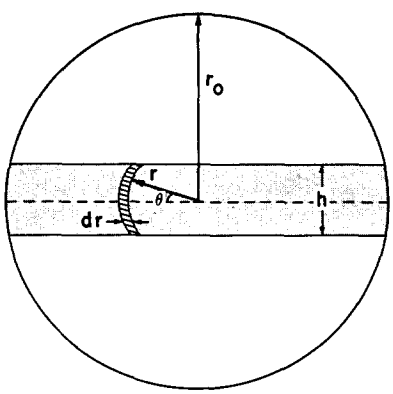


FIG. 1. Cross-sectional view of flow tube illustrating the geometry germane to the radial number-density gradient problem. The shaded area approximates the monochromator's field of view.

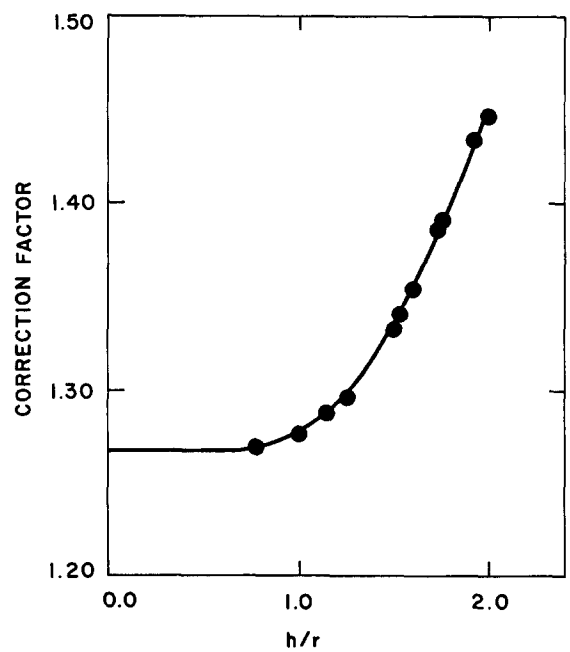


FIG. 2. Variation in the correction factor for energy pooling measurements with the ratio $h/r$.

in steady state in our reactor so that we can equate its formation and decay rates. Thus we have

$$\frac{d[N_2(C,v)]}{dt} = 1.267 \sum_{v'} \sum_{v''} k^{C,v}_{v'v''} [N_2(A,v')] \times [N_2(A,v'')] - k^{C,v}_{\text{rad}} [N_2(C,v)] = 0, \tag{14}$$

$$[N_2(C,v)] = 1.267 \sum_{v''} \sum_{v'} \frac{k^{C,v}_{v'v''}}{k^{C,v}_{\text{rad}}} [N_2(A,v')][N_2(A,v'')]. \tag{15}$$

For the case of only one vibrational level of $N_2(A)$, Eq. (15) collapses to a single term for which the $N_2(C)$ number density varies linearly with the square of the $N_2(A)$ number density. The slope will equal the ratio of the energy-pooling rate coefficient to the radiative-decay rate of $N_2(C)$.

Figures 3 and 4 show representative spectra of the 220 to 400 nm region which encompasses most of the major emissions in the $N_2(A$–$X)$ and $N_2(C$–$B)$ systems. Comparison of the two figures shows how strongly the $N_2(C)$ intensity varies with the $N_2(A)$ intensity. Figures 5 and 6 show typical plots of the variation in the number density of $N_2(C,v')$ as a function of the square of the $N_2(A)$ number density under conditions where only $v' = 0$ of the $A$ state was in the reactor.

If only vibrational levels of 0 and 1 of $N_2(A)$ are present, Eq. (15) becomes

$$[N_2(C,v)] = 1.267 \frac{k^{C,v}_{00}}{k^{C,v}_{\text{rad}}} [N_2(A,v'=0)]^2 + 2.534 \frac{k^{C,v}_{01}}{k^{C,v}_{\text{rad}}} \times [N_2(A,v'=0)][N_2(A,v'=1)] + 1.267 \frac{k^{C,v}_{11}}{k^{C,v}_{\text{rad}}} [N_2(A,v'=1)]^2. \tag{16}$$

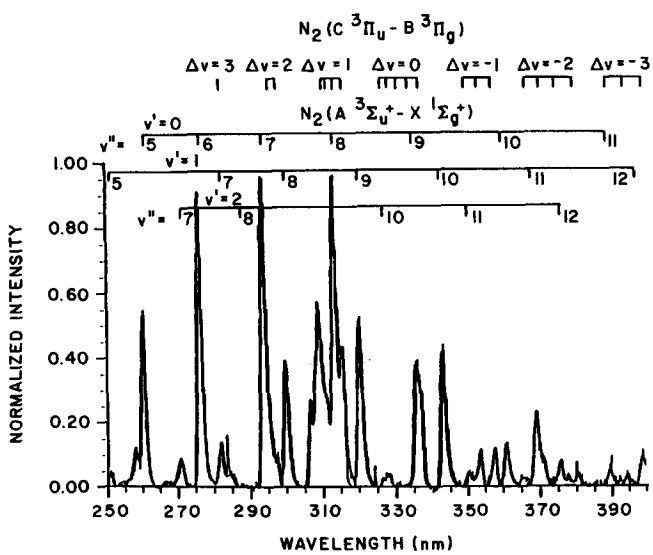


FIG. 3. Observed (heavy line) and computed best fit (light line) to the spectral region between 250 and 400 nm. Resolution 1.0 nm. Full scale sensitivity 1 kHz.

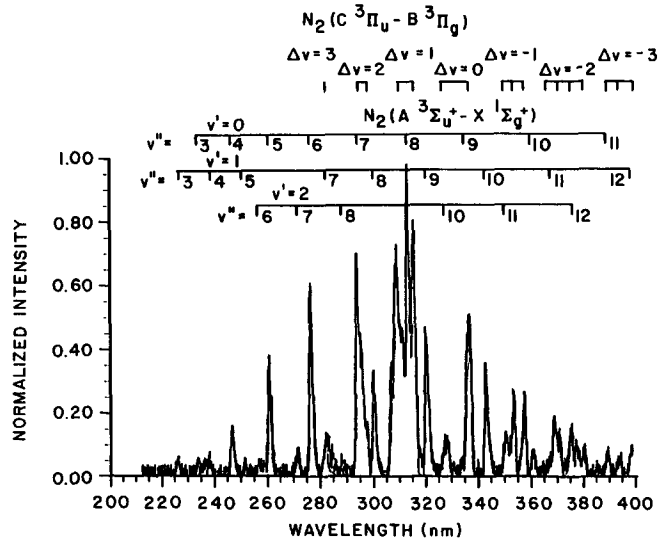


FIG. 4. Observed (heavy line) and computed best fit (light line) to the spectral region between 220 and 400 nm. Resolution 1.0 nm. Full scale sensitivity 3 kHz.

Dividing this equation through by $[N_2(A,v'=0)]^2$ gives a quadratic equation in the parameter $[N_2(A,v'=1)]/[N_2(A,v'=0)]$:

$$\frac{[N_2(C,v)]}{[N_2(A,v'=0)]^2} = 1.267 \frac{k^{C,v}_{00}}{k^{C,v}_{\text{rad}}} + 2.534 \frac{k^{C,v}_{01}}{k^{C,v}_{\text{rad}}} \frac{[N_2(A,v'=1)]}{[N_2(A,v'=0)]} + 1.267 \frac{k^{C,v}_{11}}{k^{C,v}_{\text{rad}}} \left\{ \frac{[N_2(A,v'=1)]}{[N_2(A,v'=0)]} \right\}^2. \tag{17}$$

Figures 7 and 8 show data plotted in this fashion for two $N_2(C)$ vibrational levels excited in the energy-pooling reaction. The most interesting thing these plots show is the absence of a significant quadratic term. The intercepts of the plots, of course, give rate coefficients that agree with those previously determined from studying just $v' = 0$ pooling. Table I summarizes the results of $N_2(C)$ energy-pooling studies.

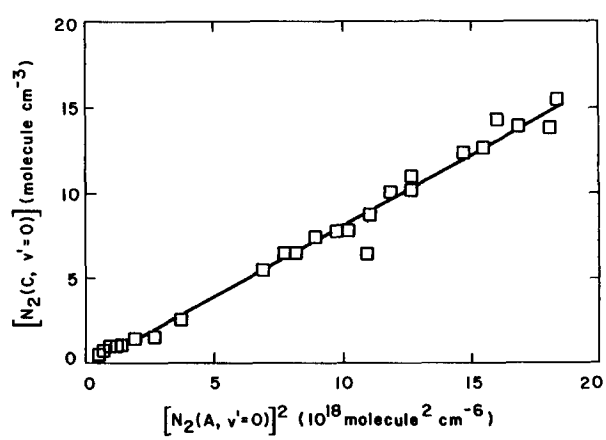


FIG. 5. Variation in the number density of $N_2(C,v' = 0)$ as a function of the square of the number density of $N_2(A,v' = 0)$.

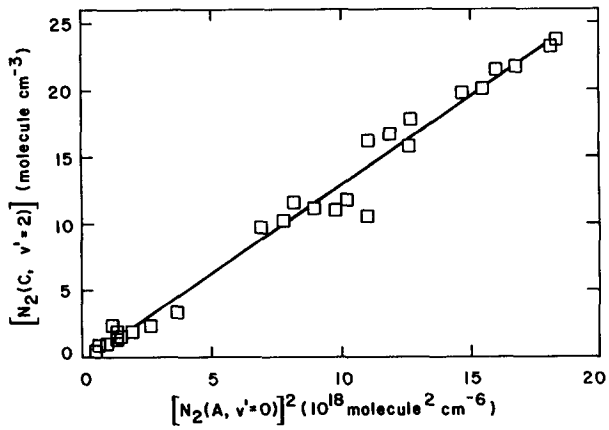


FIG. 6. Variation in the number density of $N_2(C,v'=2)$ as a function of the square of the number density of $N_2(A,v'=0)$.

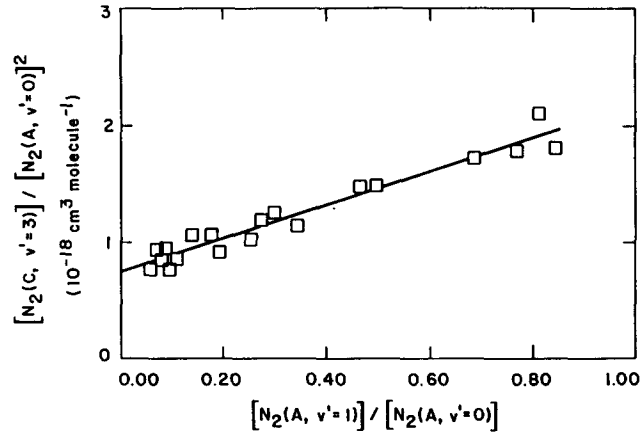


FIG. 8. Variation of the ratio of the number density of $N_2(C,v'=3)$ to the square of the number density of $N_2(A,v'=0)$ as a function of the ratio of the number densities of vibrationally excited to unexcited $N_2(A)$.

## B. Herman infrared formation from $N_2(A)$ energy pooling

The Herman infrared system was first observed 35 years ago by Herman.[32] Subsequent spectroscopic work on the system has failed to identify either the upper or lower states in the transition,[33–35] although Nadler and Rosenwaks[8] have been able to establish an upper limit to the upper state term energy of 12.02 eV. Nadler and Rosenwaks have discussed the identification of the two states and concluded the lower state might be the $G\,^3\Delta_g$ state, the lower state of the Gaydon–Herman Green system, and that the upper state was a $^3\Pi_u$ state which is known only through Michael's calculations.[36] Gilmore[37] and Michaels[38] both dispute these identifications, however. Gilmore suggests $C''\,^5\Pi_u$ and $A'\,^5\Sigma_u^+$ as the upper and lower states, respectively.[37]

Figures 9 and 10 show the HIR system excited in energy pooling of $N_2(A,v'=0)$ and $N_2(A,v'=0,1)$, respectively. The spectra were taken at 7.5 Torr total pressure with a nitrogen partial pressure of 1.5 Torr. Thus, nitrogen first-positive emission is virtually absent from the spectrum. The ratio of the HIR intensity to the square of the $N_2(A)$ number density does not vary with pressure.[6] Thus, the state is not quenched electronically under our conditions, and a steady-state analysis similar to that given above for the $N_2(C)$ state applies here. We write

$$I_{\mathrm{HIR}} = k_{\mathrm{rad}}^{\mathrm{HIR},3}[\mathrm{HIR},v'=3]$$
$$= 1.267 k_{00}^{\mathrm{HIR},3}[N_2(A,v'=0)]^2. \quad (18)$$

Figure 11 shows data for $v'=3$ of the HIR system plotted this way. For these studies, $CF_4$ or $CH_4$ was added to the reactor to relax the $N_2(A)$ vibrational energy to $v'=0$. From the slope of the plot, we find that the rate coefficient for producing $v'=3$ of the HIR system in the energy pooling of two $N_2(A,v'=0)$ molecules is $8.1\times10^{-11}$ cm$^3$ molecule$^{-1}$ s$^{-1}$. Strictly speaking, this figure is a lower limit, because other transitions of the HIR system from $v'=3$ might appear outside the bandpass of our detection system. The relative intensities of the four bands we do see, however, indicate that we have sampled both sides of the Condon parabola. Thus in all probability, we have observed the major emissions from $v'=3$. When the $N_2(A)$ was vibrationally excited, the ratio of the HIR $v'=3$ intensity to the square of the $N_2(A,v'=0)$ number density remains constant. Thus, vibrationally excited $N_2(A)$ appears not to play any role in exciting HIR, $v'=3$ from energy pooling.

Under conditions where only $v'=0$ and 1 of the $N_2(A)$ are present, we also see emission from $v'=2$ of the HIR

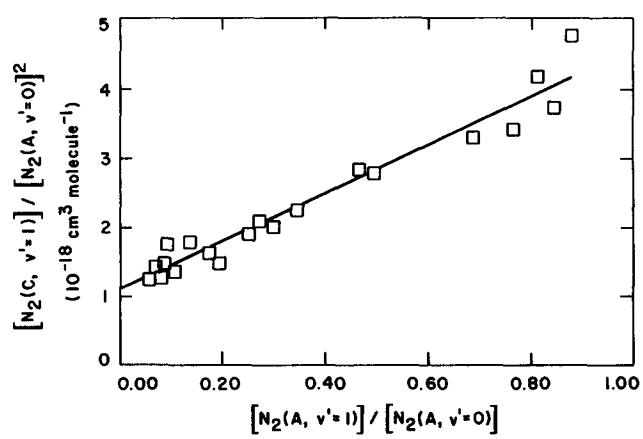


FIG. 7. Variation in the ratio of the number density of $N_2(C,v'=1)$ to the square of the number density of $N_2(A,v'=0)$ as a function of the ratio of the number densities of vibrationally excited to unexcited $N_2(A)$.

TABLE I. Rate coefficients for $N_2(C\,^3\Pi_u)$ formation from $N_2(A\,^3\Sigma_u^+)$ energy pooling.[a]

| $N_2(C,v')$ | $k_{00}^{C,v'}$ | $k_{01}^{C,v'}$ | $k_{11}^{C,v'}$ |
|---|---|---|---|
| 0 | $2.6\pm0.1$ | $3.4\pm0.7$ | $<1.0$ |
| 1 | $4.1\pm0.2$ | $5.4\pm1.2$ | $<2.0$ |
| 2 | $4.1\pm0.2$ | $3.3\pm0.8$ | $<1.0$ |
| 3 | $2.8\pm0.2$ | $2.2\pm0.5$ | $<0.7$ |
| 4 | $1.0\pm0.1$ | $1.0\pm0.6$ | $<0.6$ |
| Total $N_2(C)$ | $14.6\pm0.8$ | $15.3\pm3.8$ | $<5.3$ |

[a] Rate coefficients are in units of $10^{-11}$ cm$^3$ molecule$^{-1}$ s$^{-1}$. Error bars represent $2\sigma$ statistical uncertainties in fits. Total uncertainties are $\approx30\%$.

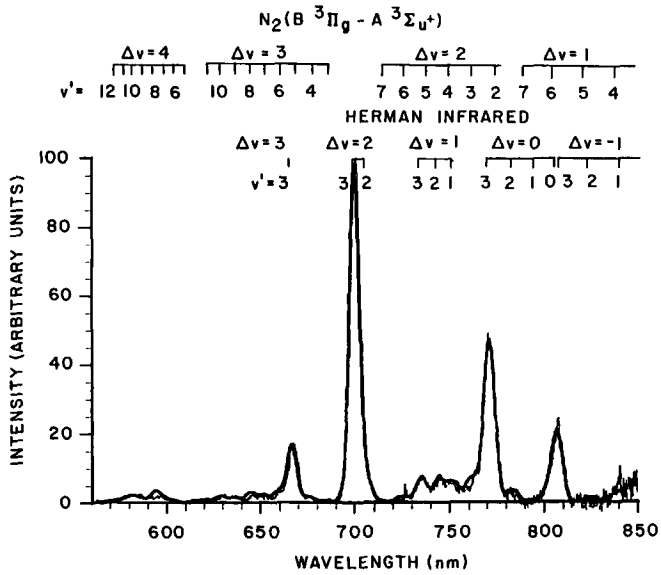


FIG. 9. Spectrum of the Herman infrared $v' = 3$ system (light line) excited in the energy pooling of $N_2(A,v' = 0)$. The heavy line is the synthetic fit to the spectrum. $P_{\text{total}} = 7.5$ Torr, $X_{N_2} = 0.20$.

system. The lower two vibrational levels of the HIR system appear only when the number densities of $v' = 2$ and 3 of the $N_2(A)$ become important. We can analyze the HIR $v' = 2$ data in a similar fashion to our analysis for vibrational effects in $N_2(C)$ production, but since we already know that two $v' = 0$ molecules do not pool to make an HIR $v' = 2$ molecule, we can eliminate the first term in the equation. Thus,

$$I^{\text{HIR},2} = 2.534k_{01}^{\text{HIR},2}[N_2(A,v' = 0)][N_2(A,v' = 1)] + 1.267k_{11}^{\text{HIR}}[N_2(A,v' = 1)]^2, \quad (19)$$

$$\frac{I^{\text{HIR},2}}{[N_2(A,v' = 0)][N_2(A,v' = 1)]} = 2.534k_{01}^{\text{HIR},2} + 1.267k_{11}^{\text{HIR},2}\frac{[N_2(A,v' = 1)]}{[N_2(A,v' = 0)]}. \quad (20)$$

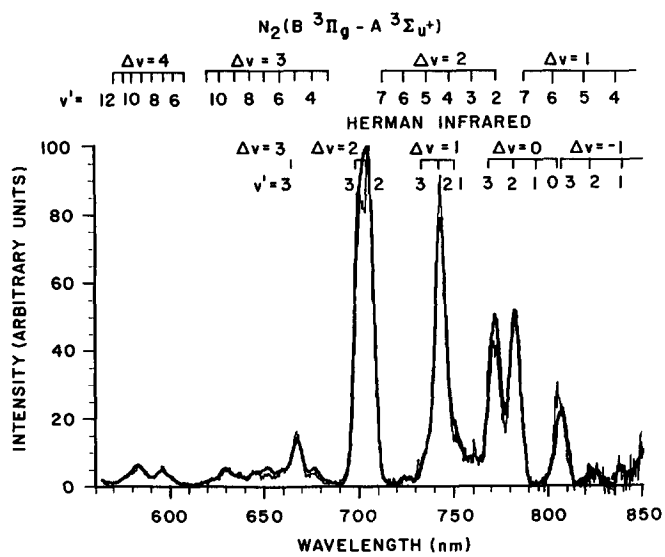


FIG. 10. Spectrum of the Herman infrared $v' = 2,3$ systems (light line) excited in the energy pooling of $N_2(A,v' = 0,1)$. The heavy line is the synthetic fit to the spectrum. $P_{\text{total}} = 7.5$ Torr, $X_{N_2} = 0.20$.

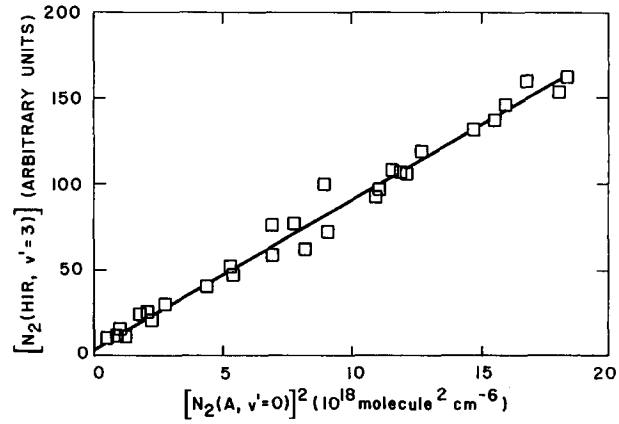


FIG. 11. Variation in the number density of $N_2(HIR,v' = 3)$ as a function of the square of the number density of $N_2(A,v' = 0)$.

Figure 12 shows the data for the HIR $v' = 2$ system. The intercept of the plot, after application of the appropriate corrections, gives the value for the mixed $v' = 0/v' = 1$ pooling rate coefficient, $9.9\times10^{-11}$ cm$^3$ molecule$^{-1}$ s$^{-1}$. Within statistical uncertainty, the linear term is not significant, again implying that energy pooling by two $v' = 1$ molecules is negligible. Table II summarizes our results on the Herman infrared system. Our data further show that HIR $v' = 2$ is not formed by pooling of vibrational levels of $N_2(A)$ higher than $v' = 1$. We have yet to collect adequate data on the formation of HIR $v' = 0,1$ which is formed in pooling of $N_2(A,v' \geqslant 2)$.

## IV. DISCUSSION

Hays and Oskam,[3] in a pulsed, static discharge, measured a rate coefficient for $N_2(C)$ energy pooling of $2.6^{+2}_{-1.4}\times10^{-10}$ cm$^3$ molecule$^{-1}$ s$^{-1}$. Within experimental error, our values agree adequately. They reported a relative $N_2(C)$ vibrational distribution of 100:92:72:50:47 for vibrational levels 0–4, respectively. Their $N_2(A)$ vibrational distribution was 100:250:80, for vibrational levels 0–2, respectively. For an $N_2(A)$ $v' = 1/v' = 0$ ratio of 3/1, our results would predict an $N_2(C)$ vibrational distribution of 100:160:110:70:30, in disagreement with Hays and Oskam's result.

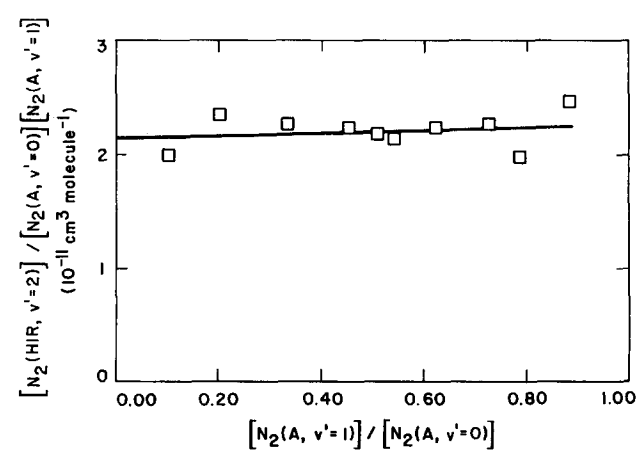


FIG. 12. Variation in the ratio of the $N_2(HIR,v' = 2)$ number density to the product of the number densities of $N_2(A)$ $v' = 0$ and $v' = 1$ as a function of the ratio of the number densities of $N_2(A)$ $v' = 1$ to $v' = 0$.

TABLE II. Rate coefficients for Herman infrared formation from $N_2(A)$ energy pooling.[a]

| HIR,$v'$ | $k_{00}$ | $k_{01}$ | $k_{11}$ |
|---|---|---|---|
| 3 | $>8.1 \pm 0.4$ | ... | ... |
| 2 | ... | $>9.9 \pm 1.0$ | ... |

[a] Rate coefficients are in units of $10^{-11}$ cm$^3$ molecule$^{-1}$ s$^{-1}$. Error bars represent $2\sigma$ statistical uncertainty in fits. Total uncertainty is $\approx 30\%$.

Applying our measured rate coefficients to Clark and Setser's[5] 0.61/1 ratio for $N_2(A)$ $v' = 1/v' = 0$, gives an overall rate coefficient of $1.3 \times 10^{-10}$ cm$^3$ molecule$^{-1}$ s$^{-1}$, about 60% of their value. Some of this discrepancy results from their not including the 27 to 45% correction for radial density gradient effects in their analysis. Additionally, their measurements may be contaminated by scattered second-positive emission from their discharge. They reported a $N_2(C)$ vibrational distribution of 100:89:70 for $v' = 0$–2, respectively, in contrast to our measured value of 100:160:120. Scattered light will enhance $v' = 0$ relative to the other vibrational levels. Subsequent measurements by Nadler *et al.*[6] found a distribution of $100 \pm 4{:}125 \pm 6{:}81 \pm 4{:}62 \pm 12{:}62 \pm 25$. They used the reaction between metastable Xe atoms and nitrogen as their $N_2(A)$ source, thereby eliminating the possibility of scattered light contamination. Their $N_2(A)$ vibrational distribution was unspecified, although they did state that most of their $N_2(A)$ was in vibrational levels 0 and 1. Assuming their $N_2(A)$ vibrational distribution was similar to Clark and Setser's, then the vibrational distribution calculated from our data for comparison with that of Nadler *et al.* would be $100 \pm 9{:}157 \pm 16{:}119 \pm 12{:}81 \pm 7{:}32 \pm 7$, in modest accord with the results of those authors. Their distribution concurs better with what we observe when the $N_2(A)$ is somewhat hotter vibrationally. Under conditions such that only 30 to 45% of the $N_2(A)$ is in $v' = 0$, our $N_2(C)$ vibrational distribution is $100 \pm 7{:}140 \pm 7{:}110 \pm 15{:}70 \pm 10{:}45 \pm 10$.

Nadler and Rosenwaks[8] studied the energy pooling of $N_2(A)$ in some detail, and noted how the vibrational distribution of $N_2(A)$ affected the vibrational distribution in the product $N_2(C)$ and Herman infrared systems. They report a vibrational distribution of $100 \pm 3{:}150 \pm 7{:}137 \pm 5{:}151 \pm 2{:}27 \pm 7$ for $N_2(C,v' = 0-4)$, respectively, formed from energy pooling between $N_2(A,v' = 0)$ molecules only. This agrees moderately well with our observations which give an $N_2(C)$ vibrational distribution of $100 \pm 4{:}158 \pm 8{:}158 \pm 8{:}108 \pm 8{:}38 \pm 4$ from $N_2(A,v' = 0)$ energy pooling. When the $N_2(A)$ was vibrationally excited, such that 60% of it was in vibrational levels 1 and above, their $N_2(C)$ distribution was $100 \pm 3{:}130 \pm 5{:}95 \pm 4{:}99 \pm 4{:}40 \pm 5$. As noted above, we observe a similar $N_2(C)$ vibrational distribution with the vibrationally hotter $N_2(A)$. In terms of distributions, our only significant disagreement with the observations of Nadler and Rosenwaks is that they report about 40% more excitation of $N_2(C,v' = 3)$ for formation from both vibrationally excited and vibrationally cold $N_2(A)$. One intriguing finding of both studies is that the product $N_2(C)$ is more vibrationally excited when the $N_2(A)$ is not and vice versa. Table III summarizes these comparisons between literature reports.

Nadler and Rosenwaks tried to rationalize their observations with a simple model which essentially is the combination of simple Franck–Condon and minimum-energy-defect models. Thus they posited that the $N_2(C)$ vibrational level populations would follow a distribution determined by the product of the Franck–Condon factors for the transitions from one of the $N_2(A)$ molecules to the $C$ state and the other one to the $X$ state times $\exp(-|\Delta E|/kT)$ where $|\Delta E|$ is the magnitude of the energy defect in the energy transfer reaction. Because our results are essentially state-to-state observations, we can test this model in some detail. Table IV compares the calculated and observed state-to-state energy pooling rate coefficients for the cases of two $N_2(A,v' = 0)$ molecules, $N_2(A,v' = 0)$ with $N_2(A,v' = 1)$, and two $N_2(A,v' = 1)$ molecules. The calculated values have been normalized so that the sum of the rate coefficients for two

TABLE III. Comparison between results of various groups on $N_2$ excitation by $N_2(A)$ energy pooling.

| Group | Relative $N_2(A)$ populations | | | | Relative $N_2(C)$ populations | | | | | Total rate[a] coefficient |
|---|---|---|---|---|---|---|---|---|---|---|
| | $v' = 0$ | 1 | 2 | 3 | $v = 0$ | 1 | 2 | 3 | 4 | |
| Hayes and Okam[b] | 100 | 250 | 80 | | 100 | 92 | 72 | 50 | 47 | $2.6^{+2}_{-1.4}$ |
| Present results[c] | 100 | 300 | | | 100 | 160 | 110 | 70 | 30 | |
| Clark and Setser[d] | 100 | 61 | | | 100 | 89 | 70 | | | $1.8 \pm 0.2$ |
| Nadler *et al.*[e] | 100 | 61 | ? | | $100 \pm 4$ | $125 \pm 6$ | $81 \pm 4$ | $62 \pm 12$ | $62 \pm 25$ | $2.2^{f} \pm 0.3$ |
| Present results[c] | 100 | 61 | | | $100 \pm 9$ | $157 \pm 16$ | $119 \pm 12$ | $81 \pm 7$ | $32 \pm 7$ | $1.30 \pm 0.4$ |
| Nadler and Rosenwaks[g] | 100 | ... | ... | | $100 \pm 3$ | $150 \pm 7$ | $137 \pm 5$ | $151 \pm 2$ | $27 \pm 7$ | |
| Present results[c] | 100 | ... | ... | | $100 \pm 4$ | $158 \pm 8$ | $158 \pm 8$ | $108 \pm 8$ | $38 \pm 4$ | $1.5 \pm 0.4$ |
| Nadler and Rosenwaks[g] | 100 | 90 | 60 | $<10$ | $100 \pm 3$ | $130 \pm 5$ | $95 \pm 4$ | $99 \pm 4$ | $40 \pm 5$ | |
| Present results[h] | 100 | 80 | 50 | 18 | $100 \pm 7$ | $140 \pm 7$ | $110 \pm 15$ | $70 \pm 10$ | $45 \pm 10$ | |

[a] Units of $10^{-10}$ cm$^3$ molecule$^{-1}$ s$^{-1}$.
[b] Reference 4.
[c] Calculated from results in Table I.
[d] Reference 5.
[e] Reference 6.
[f] Estimate from Ref. 5.
[g] Reference 8.
[h] Measured values in under conditions of high $N_2(A,v)$ excitation.

TABLE IV. Comparison between observed $N_2(C\,^3\Pi_u)$ vibrational distributions excited by $N_2(A\,^3\Sigma_u^+)$ energy pooling and those calculated from a Franck–Condon model.

| | $v'=0$ | | 1 | | 2 | | 3 | | 4 | | $\Sigma k^{C,v}$ | |
|---|---|---|---|---|---|---|---|---|---|---|---|---|
| $k^{C,v}$ | Calc[a] | Obs | Calc | Obs | Calc | Obs | Calc | Obs | Calc | Obs | Calc | Obs |
| $2N_2(A,v'=0)$ | 0.14 | 2.6 | 1.3 | 4.1 | 5.7 | 4.1 | 7.3 | 2.8 | 0.10 | 1.0 | 14.5 | 14.6 |
| $N_2(A,v'=0)+N_2(A,v'=1)$ | 1.3 | 3.4 | 1.0 | 5.4 | 0.48 | 3.3 | 1.3 | 2.2 | 7.5 | 1.0 | 11.6 | 15.3 |
| $2N_2(A,v'=1)$ | 0.0004 | <1 | 7.3 | <2 | 2.8 | <1 | 0.007 | <0.7 | 0.17 | <0.6 | 10.3 | <5 |

[a] The calculated values have been normalized to give the correct total rate coefficient for $2N_2(A,v'=0)$ energy pooling.

$N_2(A,v'=0)$ molecules equals the experimentally observed rate coefficient. Clearly, the model does not do a very good job of predicting the relative vibrational distributions, how these vibrational distributions change from case to case, nor how the absolute magnitude of the vibrational distributions changes from case to case. While the model does indicate that two $N_2(A,v'=0)$ molecules excite $N_2(C,v'=2,3)$ more efficiently than is the case for vibrationally excited $N_2(A)$, it fails to predict the opposite trend for $N_2(C,v'=1,4)$. Furthermore, the model predicts very significant excitation of $N_2(C)$ in collisions with two $N_2(A,v'=1)$ molecules in disagreement with our observations. The Franck–Condon model appears to be inadequate to describe detailed interactions in this type of energy transfer reaction. We have noted such a failure previously in our studies on the excitation of NO by $N_2(A)$.[14]

Nadler and Rosenwaks also investigated the excitation of the Hermal infrared system by $N_2(A)$ energy pooling. By comparing the relative intensities of the second-positive bands and the Herman infrared bands, they estimated a lower limit to the rate coefficient for HIR formation from $N_2(A)$ energy pooling of $7\times10^{-11}$ cm$^3$ molecule$^{-1}$ s$^{-1}$. This estimate assumes a rate coefficient for $N_2(C)$ formation of $2.5\times10^{-10}$ cm$^3$ molecule$^{-1}$ s$^{-1}$. Reducing their HIR estimate by 40% to place it on the same relative basis as our $N_2(C)$ formation rate coefficients results in a value of $4\times10^{-11}$ cm$^3$ molecule$^{-1}$ s$^{-1}$ for the Nadler and Rosenwaks estimate. This is about half of what we measure directly. Nadler and Rosenwaks' estimate is based upon a Herman infrared spectrum which is much more contaminated by first-positive emission than is our spectrum. Thus the HIR intensities would have been much more difficult for them to estimate. We also do not agree with them on some of the details of the HIR vibrational distribution produced by $N_2(A)$ energy pooling. We do not see any convincing evidence for formation of $N_2(\mathrm{HIR},v'=0,1)$ from the pooling of two $N_2(A,v'=0)$ molecules, whereas Nadler and Rosenwaks report that the intensities of emissions from these two levels drops by a factor of only about 2 in going from unrelaxed to vibrationally relaxed $N_2(A)$. Both studies clearly do show a strong enhancement of $N_2(\mathrm{HIR},v'=3)$ when only $N_2(A,v'=0)$ is present in the reactor, and both note an absence of $N_2(\mathrm{HIR},v'=2)$ for the case of vibrationally relaxed $N_2(A)$. In fact, we observe that the ratio of $[N_2(\mathrm{HIR},v'=3)]$ to $[N_2(A,v'=0)]^2$ remains constant under all conditions of vibrational excitation of the $N_2(A)$. Similarly, we find that the ratio of $[N_2(\mathrm{HIR},v'=2)]$ to the product $[N_2(A,v'=0)]\times[N_2(A,v'=1)]$ is invariant under all observed conditions of $N_2(A)$ vibrational excitation. This includes cases in which 70% of the $N_2(A)$ is vibrationally excited. Under conditions of moderate vibrational relaxation of the $N_2(A)$, however, conditions where only the two lowest vibrational levels are in the reactor, we also fail to see any evidence of $N_2(\mathrm{HIR},v'=0,1)$. Only under conditions such that vibrational levels 2 and above exist in the reactor do we see any emission from the two lowest HIR vibrational levels. Under such conditions, the HIR spectra are severely overlapped by first positive emission, and difficult to analyze. Thus, we have as yet made no quantitative estimates of the rate coefficients for producing these two lowest levels of the HIR system from $N_2(A)$ energy pooling.

## V. SUMMARY AND CONCLUSIONS

We have reported state-to-state rate coefficients for excitation of $N_2(C\,^3\Pi_u)$ and the $N_2$ Herman infrared system in $N_2(A\,^3\Sigma_u^+)$ energy pooling. Our results show that the energy pooling process is essentially gas kinetic, and that the final vibrational state distributions depend strongly upon the initial $N_2(A)$ vibrational distributions. This product-state selectivity is particularly striking in the case of Herman infrared excitation where specific combinations of $N_2(A)$ states produce only one of the available HIR states. A model combining Franck–Condon overlap with minimum energy defect is inadequate to predict the observed distributions. Presumably, one must look at specific potential curve crossings in detail to understand these phenomena.

Observations of the formation of $N_2(B\,^3\Pi_g)$ from $N_2(A)$ energy pooling[39] result in rate coefficients similar in magnitude to those observed here, and also show some unusual state specificity. Taken together, our results would support a total rate coefficient for $N_2(A)$ energy pooling of $(3–4)\times10^{-10}$ cm$^3$ molecule$^{-1}$ s$^{-1}$, substantially lower than some previous suggestions which have exceeded $10^{-9}$ cm$^3$ molecule$^{-1}$ s$^{-1}$.[3,7] We will discuss the $N_2(B)$ formation results and their implications regarding the total $N_2(A)$ energy pooling rate coefficient in a future publication.

## ACKNOWLEDGMENTS

We appreciate partial support for this work from the Defense Nuclear Agency (Project 5A, Task 5A, Work Unit 115) and the Air Force Office of Scientific Research (Task 2310G4) through Air Force Geophysics Laboratory Contract No. F19628-85-C-0032 and from the Air Force Wea-

pons Laboratory under Contract No. F29601-84-C-0076. We enjoyed interesting discussions with Dave Green and Terry Rawlins (PSI), Don Setser (KSU), Forrest Gilmord (RDA) and Harvey Michaels (UTRC), and appreciated Margrethe DeFaccio and Lauren Cowles' instrumental contributions to the data analysis.

[1]D. H. Stedman and D. W. Setser, Chem. Phys. **50**, 2256 (1969).
[2]G. N. Hays, C. J. Tracy, A. R. Demonchy, and H. J. Oskam, Chem. Phys. Lett. **14**, 352 (1972).
[3]G. N. Hays and H. J. Oskam, J. Chem. Phys. **59**, 1507 (1973).
[4]G. N. Hays and H. J. Oskam, J. Chem. Phys. **59**, 6088 (1973).
[5]W. G. Clark and D. W. Setser, J. Phys. Chem. **84**, 2225 (1980).
[6]I. Nadler, D. W. Setser, and S. Rosenwaks, Chem. Phys. Lett. **72**, 536 (1980).
[7]I. Nadler, A. Rotem, and S. Rosenwaks, Chem. Phys. **69**, 375 (1982).
[8]I. Nadler and S. Rosenwaks, J. Chem. Phys. **83**, 3932 (1985).
[9]L. G. Piper (unpublished results, 1980).
[10]L. G. Piper, G. E. Caledonia, and J. P. Kennealy, J. Chem. Phys. **74**, 2888 (1981).
[11]L. G. Piper, G. E. Caledonia, and J. P. Kennealy, J. Chem. Phys. **75**, 2847 (1981).
[12]L. G. Piper, W. J. Marinelli, W. T. Rawlins, and B. D.Green, J. Chem. Phys. **83**, 5602 (1985).
[13]L. G. Piper and W. T. Rawlins, J. Phys. Chem. **90**, 320 (1986).
[14]L. G. Piper, L. M. Cowles, and W. T. Rawlins, J. Chem. Phys. **85**, 3369 (1986).
[15]L. G. Piper, M. E. Donahue, and W. T. Rawlins, J. Phys. Chem. **91**, 3883 (1987).
[16]L. G. Piper, J. Chem. Phys. **87**, 1625 (1987).
[17]D. W. Setser, D. H. Stedman, and J. A. Coxon, J. Chem. Phys. **53**, 1004 (1970).
[18]D. H. Stedman and D. W. Setser, Chem. Phys. Lett. **2**, 542 (1968).
[19]N. Sadeghi and D. W. Setser, Chem. Phys. Lett. **82**, 44 (1981).
[20]A. Fontijn, A., C.B. Meyer, and H. I. Schiff, J. Chem. Phys. **40**, 64 (1964).
[21]M. Vanpee, K. D. Hill, and W. R. Kineyko, AIAA J. **9**, 135 (1971).
[22]M. F. Golde, A. E. Roche, and F. Kaufman, J. Chem. Phys. **59**, 3953 (1973).
[23]D. Golomb and J. H. Brown, J. Chem. Phys. **63**, 5246 (1975).
[24]G. A. Woolsey, P. H. Lee, and W. D. Slafer, J. Chem. Phys. **67**, 1220 (1977).
[25]M. Sutoh, Y. Morioka, and M. Nakamura, J. Chem. Phys. **72**, 20 (1980).
[26]A. M. Pravilov and L. G. Smirnova, Kinet. Catal. **19** 202 (1978).
[27]F. Kaufman, Proc. R. Soc. London Ser. A **247**, 123 (1958).
[28]F. Kauman, in *Chemiluminescence and Bioluminescence*, edited by M. J. Cormier, D. M. Hercules, and J. Lee (Plenum, New York, 1973), pp. 83–100.
[29]D. E. Shemansky, J. Chem. Phys. **51**, 689 (1969).
[30]A. Lofthus and P. H. Krupenie, J. Phys. Chem. Ref. Data **6**, 287 (1977).
[31]E. E. Ferguson, F. C. Fehsenfeld, and A. L. Schmeltkopf, Adv. At. Mol. Phys. **V**, 1 (1970).
[32]R. Herman, C. R. Acad. Sci. Paris **233**, 738 (1951).
[33]P. K. Carroll and N. D. Sayers, Proc. Phys. Soc. London **64**, 1138 (1953).
[34]D. Pleiter, Can. J. Phys. **41**, 1245 (1963).
[35]D. Mahon-Smith and P. K. Carroll, J. Chem. Phys. **41**, 1377 (1964).
[36](a) H. H. Michaels, in *The Excited State in Chemical Physics*, edited by J. W. McGowan (Wiley, New York, 1981), Vol. II., Chap. 3; (b) H. H. Michaels (private communication to S. Rosenwaks, 1985). Cited in Ref. 8.
[37]F. R. Gilmore (private communication, 1986).
[38]H. H. Michaels (private communication, 1986).
[39]L. G. Piper, J. Chem. Phys. (submitted).